CHAPTER 6

Image based modelling and simulation of hemodynamics in static human left ventricle using CT data

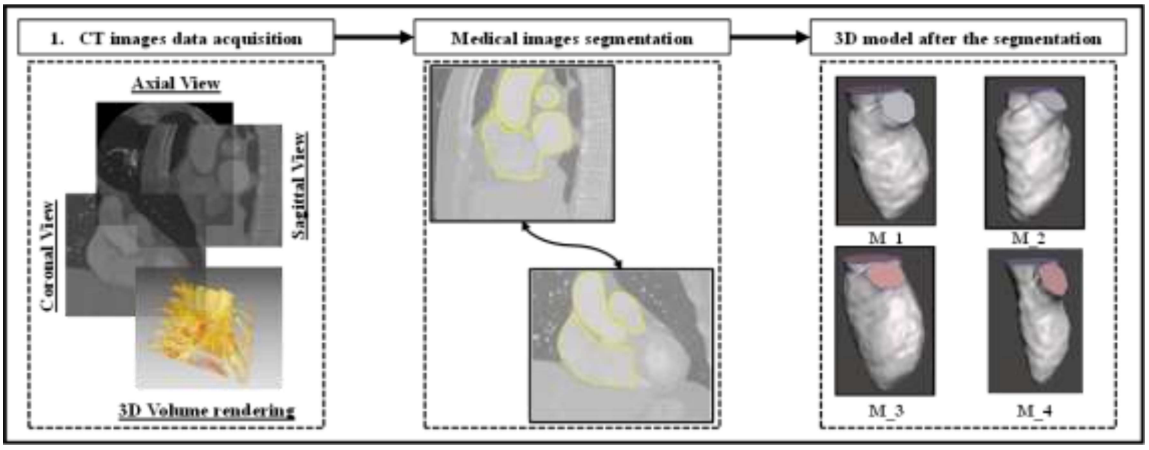

Sumit Kumar, **et al**. "Transient blood flow dynamic in 3D ellipsoidal models of LV", AIP, Physics of fluids (IF 4.98), (Under review)

Chapter 6

Image based modelling and simulation of hemodynamics in human left ventricle using CT data

6.1 Introduction

Cardiac arrest is still an utmost global threat, with an estimated prevalence of >37.7 million people around the world in 2022, and a recent report published by the World Health Organization (WHO) has shown that heart failure has increased and will rise further in the upcoming years. Heart failure will take place for a variety of reasons, such as cardiovascular disease (CVD), coronary artery disease (CAD), pulmonary heart disease (PHD), ischemic heart disease (IHD), hypertensive heart disease, and excessive blood pressure (Doost et al., 2016a; Moradi et al., 2023). The significant mortality and morbidity rates associated with CVD can be decreased with early detection and prognosis. Because of this, it is important to develop a variety of tools to help us learn more about the physiological mechanisms and events in the heart that contribute to the development and progression of different CVDs. Computational fluid dynamics (CFD) is a subset of fluid mechanics that employs various numerical methods to study the patterns and behaviors of fluid flow. CFD can provide useful hemodynamic information for the medical evaluation of heart functionality and the early detection of CVD. According to published articles (Itatani et al., 2017; Mihalef et al., 2011; Obermeier et al., 2022; Su et al., 2016), a lot of research has been done on both computational and experimental analysis of the hemodynamics of blood flow in the human heart's ventricles. The first attempt to study LV and RV hemodynamics was

made in 1970 when (Yoganathan et al., 2004) analyzed the hemodynamics in the LV. Several recent studies have used idealized models of ventricles (Corsini et al., 2014; Khalafvand et al., 2012; "Numer Methods Biomed Eng - 2014 - Khalafvand - Three-dimensional CFD MRI modeling reveals that ventricular surgical.pdf," n.d.; Yoganathan et al., 2004) or patient-specific models of healthy subject LV (physiological) to perform a numerical simulation to analyze the intraventricular blood flow patterns.

Combining patient-specific medical imaging data with CFD models of LV flow has explained promising results in getting patient-specific blood flow hemodynamics information for functional evaluation of the human heart. Segmenting the LV manually and then using different software for mesh development and registration are common first steps in the model building process. In biomedical engineering, image-based modelling of blood flow is an active field of study which depends on the heart, arteries, or veins based on images for determining patient-specific hemodynamics parameters which are not observable in vivo studies. Several authors have utilized this framework to investigate the biomechanical basis of illnesses and ways to enhance cardiovascular diagnosis and therapy. Recently, this framework has also seen widespread medical use for identifying coronary artery disease. The field of vascular medicine has been the primary focus of image-based hemodynamics modelling. Although cardiac applications do exist, they are quite rare. Despite the established role of intracardiac hemodynamics in the development of cardiovascular illness. Two basic methods exist for simulating blood flow within the heart. The first method employs time-resolved imaging to monitor cardiac deformation, and then applies that motion to the heart's

internal fluidic domains as a reference for a deforming-domain CFD issue. The second method involves solving for the heart's motion rather than measuring it by combining electrophysiology, structural mechanics, and fluid dynamics (Chen et al., 2018; Schenkel et al., 2009). Previous computational fluid dynamics (CFD) investigations of intracardiac hemodynamics have often required substantial human effort for model creation (Khalafvand et al., 2012; Salman and Yalcin, 2021). The first step in constructing a model is often the manual or semi-automated segmentation of images to define the endocardial surfaces. When studying LV hemodynamics, most studies segment not only the LV but also the inflow and outflow tracks of the left atrium and the aorta. To achieve this, we take a series of images of the heart at different intervals during the cardiac cycle and apply a segmentation algorithm to each picture. A volumetric refined mesh of the fluid domain is produced by appropriate mesh-generating software using the segmented areas at a specific time. The reference volumetric mesh is then deformed using the image segmentation process into a shape that fits within the boundaries of the mesh. These processes often involve the use of many applications, which makes data administration and organization more difficult. Furthermore, operator-dependent mistakes are unexpected, thus challenging dependability and repeatability due to the manual nature of the procedure. By manually placing seeds and segmenting the valve ring, (Schenkel et al., 2009) sped up the LV segmentation process. Using simplified LV geometries produced by a proprietary piece of software, (Nguyen et al., 2015) demonstrated a semi-automated, low-interference of operator's method for LV meshing, leveling, and restoration. While these new methods have helped speed up certain aspects of model building, they all have their drawbacks, such as relying on closed-source software or having been evaluated on just a small

sample of real-world data. Still, there is a need for an automated approach to create LV-based CFD models for patients using imaging data accurately. Increased interest in employing convolutional neural networks (CNNs) for automated dissection of cardiac configurations has followed recent advancements in deep learning. Several deep learning-based methods have worked on improving upon the segmentation accuracy of prior methods that relied on either model.

Understanding the FSI phenomena in the left heart has important clinical implications. It allows for a more accurate assessment of cardiac function and can provide insights into various cardiovascular conditions. Fluid structure interaction (FSI) analysis can help in: Patient-Specific Simulations, Hemodynamic Effects, Device Design and Evaluation and Surgical Planning. Also due to the complexity of the heart's shape, like heart's significant deformation during the cardiac cycle, the effect of the heart valves opening and closing on the heart's geometry, the electrical-fluid-structure interaction (EFSI) phenomenon involved in creating the irregular intraventricular blood flow, and the transitional blood flow between laminar and turbulent are some of the issues that have been the main topic of previously published studies (Borazjani et al., 2013; Doenst et al., 2009; Doost et al., 2016a; Xu and Kenjereš, 2021).

It is noted from the previous studies (Itatani et al., 2017)(Doost et al., 2016a) on experimental analysis using PIV and 4D-flow MRI of blood flow hemodynamics in the human heart's ventricles, that many complexities are to be considered for exact mimicking of human left ventricular blood flow. From (Figure 6.1) (Xu and Kenjereš, 2021) shows a prior work done on experimental flow patterns in the human left ventricle (LV) model with a novel dynamic mesh morphing approach based on radial

basis function. To do computational validation of these types of rigid glass-based model, mathematical modelling and simulations plays an important role. In future these types of computational modelling approach will aid in the study of patient specific problems in LV, validating heart valves function and designing a left ventricular assistive device (LVAD).

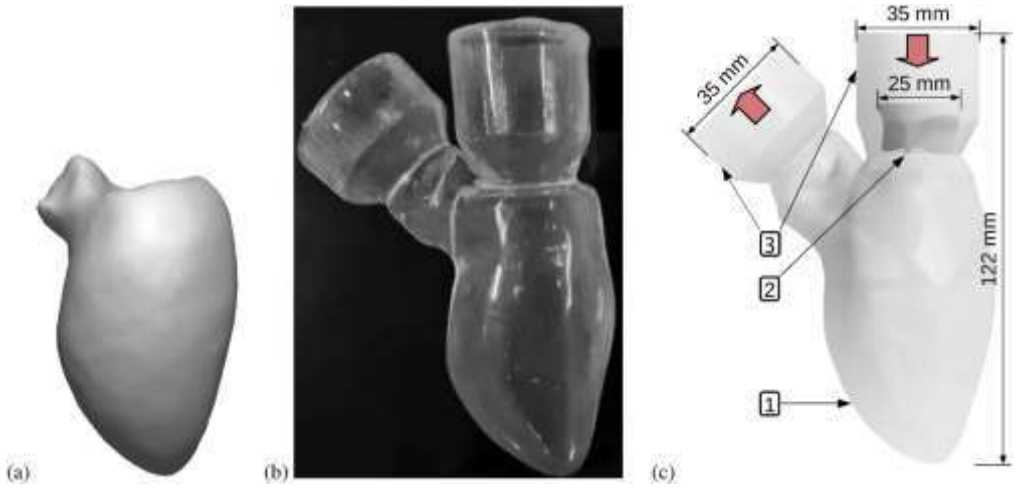

Figure 6.1: Geometrical details of the left ventricle with dynamic biological valve based on the tomographic PIV experiments (Xu and Kenjereš, 2021).

The purpose of this study is to give a technique for image-based blood flow modeling and simulation of the LV by making use of CT data. In this work due to complexity of structure, non-availability of times series cardiac scan data set and cardiac motion, the assumptions made for making CFD based hemodynamics studies are; static LV geometry, laminar flow, newtonian blood rheology material property and physiological relevant boundary conditions from literature has been considered. In this study, we employ a mixture of manual and automated-based segmentation and 3D modeling approaches to generate geometry from real-time CT data. In this study, we create and anatomically measure four distinct human LV 3D models (designated M_1, M_2, M_3,

and M_4) that faithfully reproduce the LV's intricate geometrical structure. Then, the blood velocities, streamlines, wall shear stress, vortex structures, and wall pressure in one model M_1 of the LV are analyzed using CFD during early systole and late diastole of pulsatile physiological waveform at inlet.

6.2 Methods

The proposed workflow for the modelling and simulation framework is illustrated in (Figure 6.2). For geometric modelling manual and automatic segmentation based on CT data is used. (Figure 6.2) illustrates a step-by-step methodology for computational simulations of 3D LV geometry during instantaneous diastolic phases of the cardiac cycle with pulsatile boundary conditions. The first stage contains the pre-processing, in which medical images are acquired in DICOM format; manual, & automatic segmentation using deep learning-based method and partitioning are performed to locate or extract the LV boundaries; and after segmentation, the smoothening operation is conducted to smooth the rough edges of the 3D model of the LV using (Autodesk mesh mixer). The next stage is CFD, which contains meshing, transient pulsatile boundary condition setup, and solver physics setup for simulations. The last stage is post-processing in which results extraction and analysis of hemodynamics parameters at the late diastolic and early systolic phases.

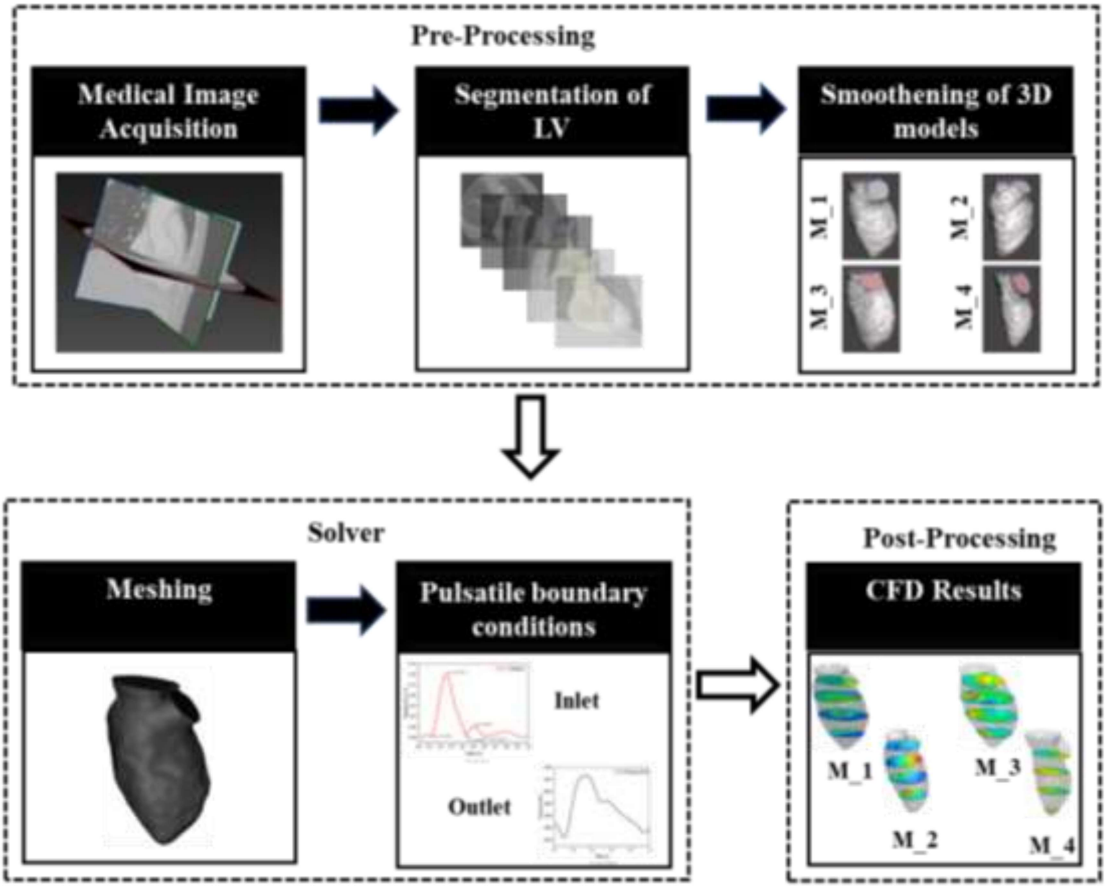

Figure 6.2 : Workflow of image based computational modelling and simulation of blood flow in the left ventricle (LV) models

6.2.1 Geometry reconstruction

Step by Step Procedure:

6.2.1.1 Image acquisition

Each medical imaging modality uses a unique physical concept to produce in vivo image data for different tissue types in a body segment. Selecting the right imaging modality is crucial for patient-specific anatomy geometric modelling. When choosing an imaging modality, consider contrast to noise ratio, signal to noise ratio, and picture artefact kinds. MRI scans, with their higher tissue resolution, are better for modelling

soft tissue. CT scans use more radiation for improved resolution but cost more and take longer than MRI scans, which also use more energy.

First, identify the organ(s)'s tissues to create a model. Then, the required picture attributes determine the medical imaging modality. The open-source multi-modality whole heart segmentation (MMWHS) challenge dataset used for modeling consists of CT or MR images of the human heart's left ventricle during one time period. CT scans show tissue pixels with linear X-ray attenuation coefficients (Su et al., 2016). The linear X-ray attenuation coefficient of air is -1000 while that of water is 0. The Hounsfield scale (HU) or CT numbers as shown in (Figure 6.3) is named after CT pioneer Godfrey Hounsfield. It quantifies radio density: can be calculated as

$$\boldsymbol{HU = 1000(\mu_X - \mu_{water})/\mu_{water}}$$

where, $\boldsymbol{\mu_X}$ Average linear attenuation coefficient in a voxel, $\boldsymbol{\mu_{water}}$ = Linear X-Ray attenuation coefficient of water.

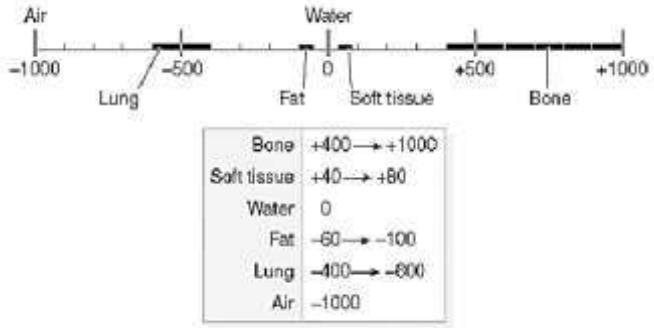

Figure 6.3: Hounsfield scale showing a range of Hounsfield Unit for body system

The axial, sagittal, and coronal body planes are oriented orthogonally to the long axis of the body for image orientation, as displayed in (Figure 6.4). These planes are utilized to generate scout images, which give a qualitative outline of heart morphology. The

axial plane can simultaneously depict the four compartments of the heart and the pericardial sac. The sagittal plane can reveal the origin of great vessels emerging in continuity from the ventricles. Whereas it is possible to evaluate the left ventricular outflow tract, the pulmonary vessels, and the left atrium using the coronal plane. However, the obliquity (45°) of these planes relative to the heart's walls prevents accurate anatomical and functional characterization. Rather, these details should be obtained from the specialized cardiac planes.

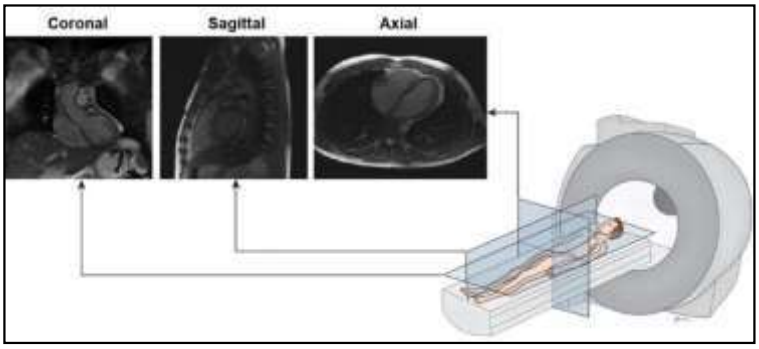

Figure 6.4 : Schematic shows orientation of major body planes with respect to patient and their corresponding appearance on bright blood imaging sequences.

The obtained images were in DICOM (Digital Imaging and Communication in Medicine) format and were easily imported into Mimics as shown in (Figure 6.5). Using CT scans, the authors of this research created a 3D model of the LV in Mimics 18.0 (Materialise, Leuven, Belgium). For surgical simulation, CFD, and FE analysis, Mimics uses 2D cross-sectional medical pictures from imaging modalities like computed tomography (CT) to construct a 3D model. The Mimics program allows for the direct import of an obtained collection of photos, most of which are in the XY plane (axial images). In addition, it performs calculations and produces pictures in the XZ

(coronal) and YZ (sagittal) axes, providing a most accurate 3D representation of the 2D data.

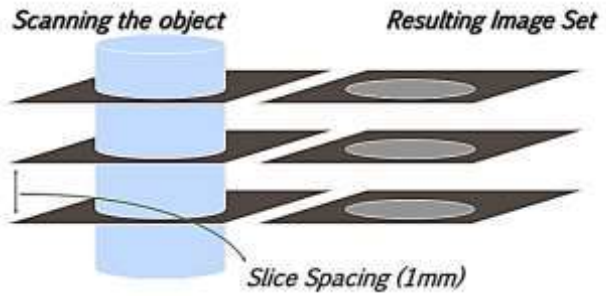

Figure 6.5 : Schematic illustrating the process of data acquisition

6.2.1.2 Preparing the acquired CT Data

The Mimics programme allows for the automated import of CT and MRI images. At this point, we changed the data's orientation after importing it using "Import Images" from the "File" menu. Correct picture presentation in MIMICS depends on the orientation parameters. It is crucial to enhance the resolution and quality of the CT images by modifying suitable acquisition parameters such as slice thickness and spatial resolution in the presence of signal noise and image distortions. Further, several methods exist for using digital image processing to improve the visual data in a picture.

- **Windowing**

Windowing is a function in Mimics that enables you to map this scale to your computer's 256 greyscale values. Windowing is a contrast adjustment technique, as shown in (Figure 6.6). Windowing is the process of altering the CT scan greyscale constituent of an image utilizing CT numbers (Hounsfield Units). It is also termed grey-level mapping, histogram alteration, contrast elongation, or contrast

enhancement. Changing windowing parameters allows us to modify/enhance the CT image's aspect and highlight specific features. Depending on the specified window, it is possible to visualize differences between soft tissues, adipose, muscles, and bones. The contrast utility comprises a grayscale with 165 predefined scales for optimal resolution.

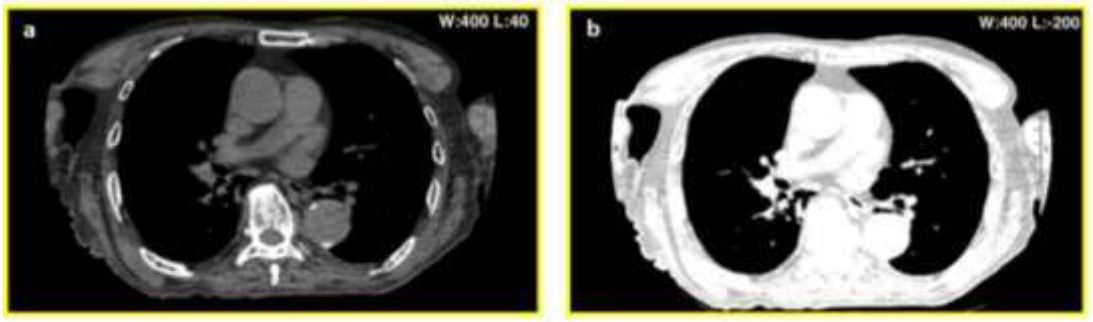

Figure 6.6 : (a) Clear distinction between a preset brighter part and grey part used to set the contrasts in Mimics 18.0 (Materialise, Leuven, Belgium)

- **Volume rendering**

Volume rendering instantly converts 2D photos into 3D models without segmentation or modelling. After visualizing, volume rendering is stopped since it delays calculation due to system memory use. The 3D visualization of volume rendering is depicted in (Figure 6.7).

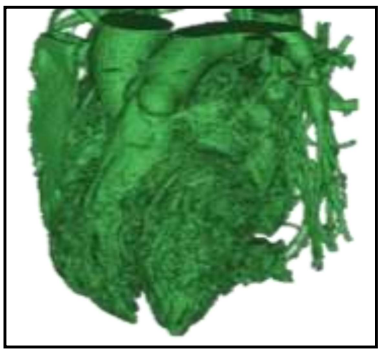

Figure 6.7 : Image showing heart scale volume rendered data

6.2.1.3 Manual segmentation and 3D model generation

All manual editing tasks include using the active mask. It was crucial to carefully study the pixels and segment them in order to maintain the original shape. Using the edit mask tool, which enables the removal, drawing, or even reestablishment of the picture with a certain threshold value, one may execute manual segmentation. This technique is used after region growth to fully segment the area of interest, producing a surface that is more continuous. In order to create a flawless 3D geometry, precise geometry may thus be retrieved from the CT scan pictures.

Segmentation is the key to converting patient physiological data from medical images to 3D models. The imported data is presented as slices that may be seen in the sagittal, frontal, and axial perspectives, respectively. Segmentation emphasizes the structure(s) or region(s) of interest in the sliced image data. Medical images created by CT or MRI scanners include grayscale data. According to the grey value (Hounsfield units in CT scans), mimics make it possible to create models from these pictures. The "grey value" is a numerical representation of the color (white, grey, or black) of a pixel in a picture. In the image data, the material density of the scanned subject is directly linked to the grey values for each pixel. Mimics may thus create models from any form that is recognizable in the scanned dataset. To create the 3D model of the LV, automatic segmentation using the threshold and region grow approach is first carried out, then manual segmentation and smoothing.

- **Threshold**

Segmenting image data and creating models is possible by grouping pixels with similar grey values. Thresholding is a segmentation technique that yields reliable models. Due to the fact that CT pictures of various anatomies will have distinctively varied grey values, it is essential to establish the threshold value accurately. After determining the cutoff value, we will be able to use CT scans to inspect the relevant subset of the recovered institutions. A low threshold helps filter out unwanted background noise. Approximately 270 on the Hounsfield scale is a good threshold for Mimics. (Figure 6.8) shows the thresholding process graphically. In the thresholding process classifying pixels within a hounsfield range depicts the same mask information. The threshold toolbar lets you choose from predefined scales for use with a number of different types of biological data. Soft tissue segmentation uses a lower threshold, whereas bone segmentation uses a higher threshold. To examine how various thresholds, bring attention to distinct parts of a picture, we employ threshold values. The cardiac (CT) technique benefits from a soft threshold in the range of 423 to 3071.

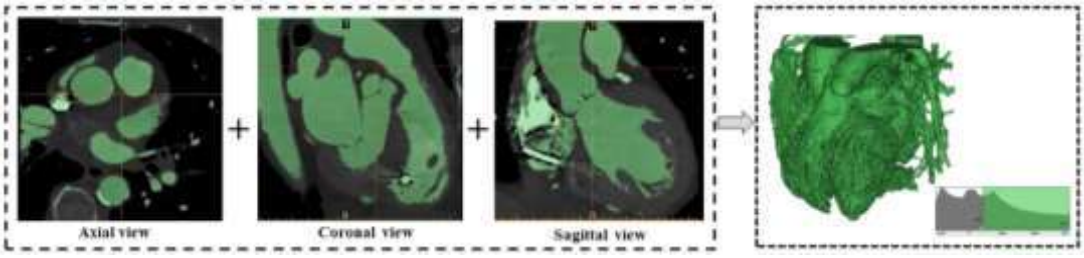

Figure 6.8 : CT images of heart are threshold with soft tissue (CT) scale. (a) Axial (b) Coronal (c) Sagittal View.

- **Region Growing**

It is an automatic partial segmentation procedure that divides masks into fragments and removes stray pixels in order to acquire the desired region, as displayed in (Figure 6.9) Since the complete segmentation cannot be provided in a single phase, the region-growing segmentation is an important step, as it enhances the portions near the complex regions with a new mask so that the entire region of interest can be visualized correctly. This makes the subsequent manual segmentation step much simpler.

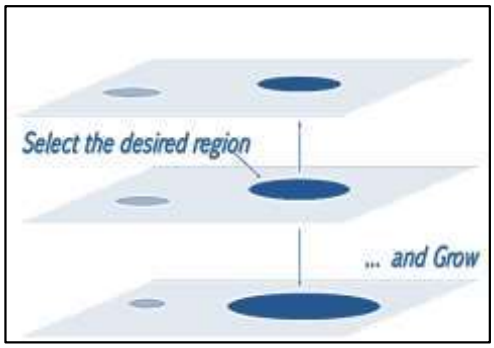

Figure 6.9: Illustration of the region grow process

- **Calculate 3D**

Mimics can use the segmentation and known information like the size of the pixels and the space between picture slices to build a 3D model. The accuracy of a scanned object is the same as the accuracy of a Mimics model. Here are the faces made with the lower and higher thresholds described above. We chose the mask we wanted to use to make the 3D model. To turn the region-grown mask into a 3D model, the best quality was chosen. (Figure 6.10) shows that a 3D model was made with a red mask to show the full shape of the LV, aorta and LA.

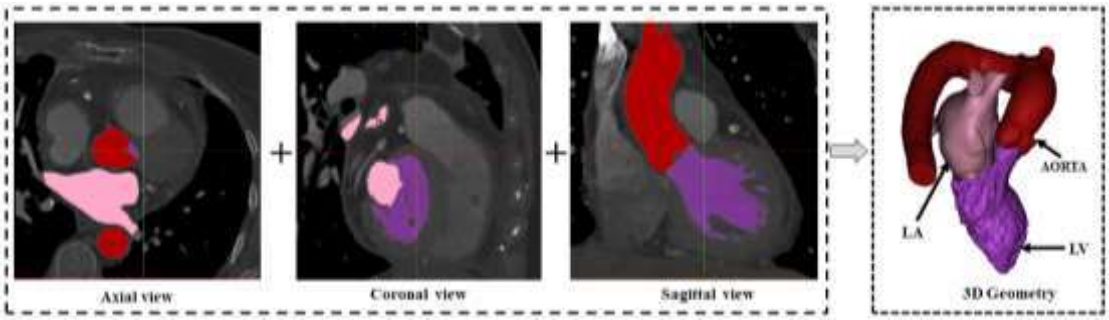

Figure 6.10 : 2D CT images converted to 3D model using manual segmentation process

- **Smoothing**

Since the model made by the above process is not accurate and has a rough surface with spikes, a smoothing operation is used to make a smooth model. Setting a smooth factor between 0 and 1 starts the iteration process. At last, the correct 3D model is made.

6.2.1.4 Automatic segmentation and 3D model generation (Deep learning method)

Automatic Segmentation Using an Ensemble of Convolutional Neural Networks of fanwei kong. This framework used a collection of CNN models, as discussed here. utilizing the input images, a CNN-based algorithm calculates the possibility that every pixel in the medical image corresponds to each anatomical region (heart chambers, myocardium, aorta, and pulmonary artery). Although, due to their high memory expenditure and computational expenses, CNN-based 3D segmentation algorithms sometimes involve down sampling the input data or using a sliding-window method to minimize memory saturation. These compromises can result in segmentation results with poor spatial resolution or considerable computational complexity. It is feasible to split 3D image data into 2D slices and then put in a 2D-based algorithm on each pixel.

Nevertheless, similar 3D CNNs, 2D CNN-based algorithms need to consider the spatial link among neighboring segments, making it impossible to explore interslice data fully. The 3D segmentation depicted in Figure 6.11 (a) & (b) was produced using an ensemble of 2D CNNs to get over the memory restriction of a 3D CNN and the data loss of 2D CNNs. Deep neural network group learning can lower variance and enhance generalization to new data since it frequently exhibits significant prediction variance. By 3D image volume rendering along the sagittal, coronal, and axial planes, we were able to produce matching 2D image datasets. A CNN model was trained to estimate the possibility that each pixel corresponds to a certain cardiac structure for each 2D dataset. We divided new 3D volumes into 2D images along the axial, coronal, and sagittal axes in order to automatically segment the volume. We then used the trained 2D CNN model (Kong and Shadden, 2020) to forecast the 2D probabilities of the sliced pictures along each viewing axis. 3D prophecies were created by stacking 2D projections for segments along the same viewing axis. The final probability prediction was calculated by averaging these three 3D predictions, which were derived from distinct observing axes. The 3D anatomical domains were then determined by locating the areas with the highest possibility for each pixel value. Algorithm 1 summarizes this automatic segmentation procedure. (Figure 6.12) depicts the four 3D LV models (M_1, M_2, M_3 & M_4) generated using automatic segmentation method of (Kong and Shadden, 2020).

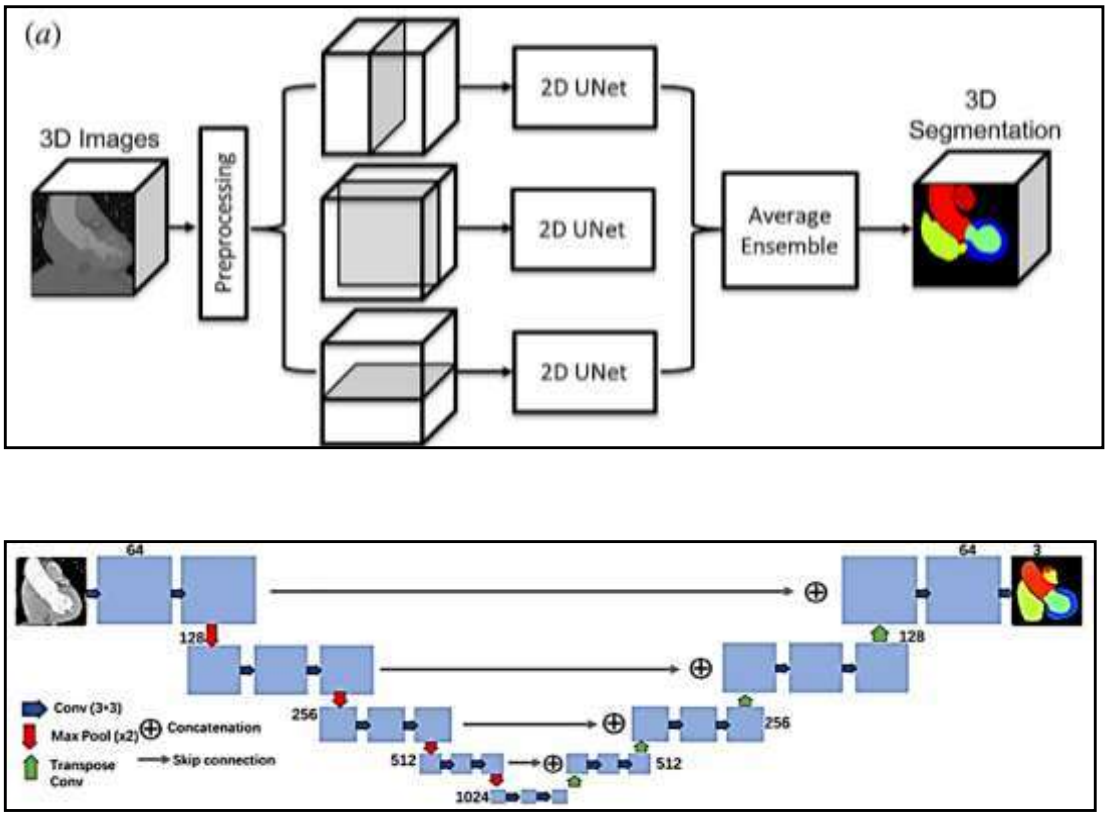

(b)

Figure 6.11: (a) Automatic segmentation workflow of the proposed approach using an ensemble of CNNs from (Kong and Shadden, 2020) (b) Network architecture of the 2D U-Net CNN model. Numbers illustrate the number of convolution kernels used.

Algorithm 1: Automatic Segmentation Using an Ensemble of CNNs (Kong and Shadden, 2020)

Input 3D CT/MR image I; 2D CNNs trained separately for three views
Output 3D segmentations S
for *each view* i **do**
  for each 2D slice s in view i **do**
  Compute the 2D probability map with the 2D CNN trained for view i
  end

Assemble 2D probability maps into a 3D probability volume Pi

$P \leftarrow P + P_i$

end

$P \leftarrow P/3$; // Compute average probability map

for *each voxel k in* S **do**

S(k) ← segmentation domain with the highest probability value in P(k)

end

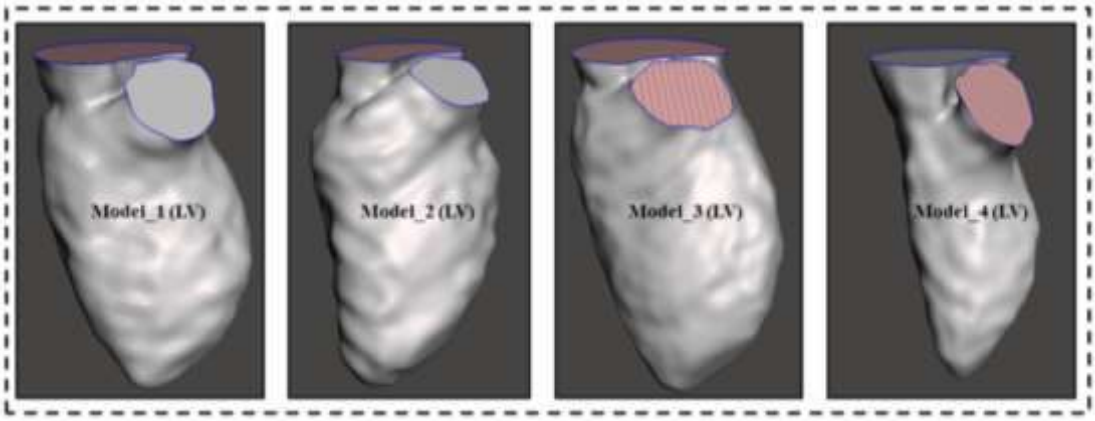

Figure 6.12: Four 3D model of LV reconstructed using automatic segmentation method

6.2.1.5 Model compatible for CFD simulations

To carry out the blood flow simulation in LV model using the CFD method, in ANSYS (Fluent) 20, firstly the STL geometry need to be made compatible for mesh generation and solver setup of the numerical modelling. Here in this work the model were converted in STEP file using Solid works. The final including inlet and outlet in the geometry on which blood flow dynamics problem was solved is shown in (Figure 6.13).

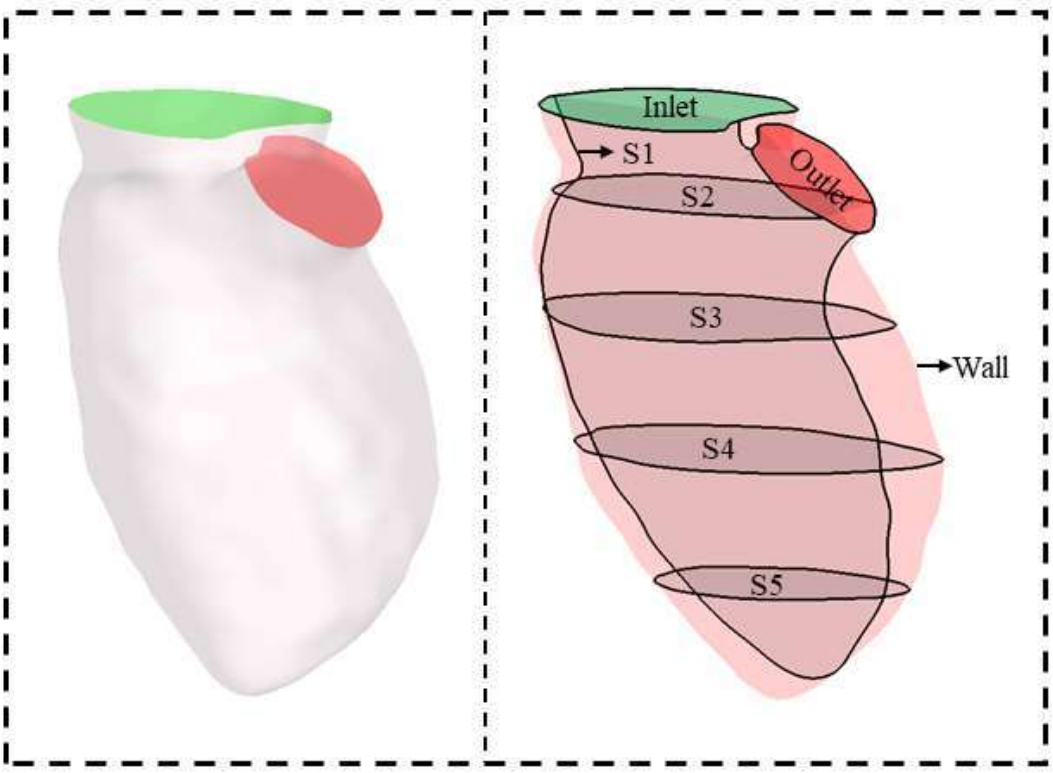

Figure 6.13 : Final ready model for CFD simulation

6.2.2 Mesh Generation

The model geometry is spatially discretized through meshing using a limited number of elements. Tetrahedral, hexahedral, or polyhedral topologies are typically utilized for mesh elements form (Khalafvand et al., 2017). In this study, 3D geometry is meshed using the fluent meshing as displayed in (Figure 6.14), and mesh parameters are described in Table.6.1. Tetrahedron mesh element is used to mesh all models due to its compatibility and ease of fits on the complex 3D shapes (Boutsianis et al., 2009c; Kadhim et al., 2018).

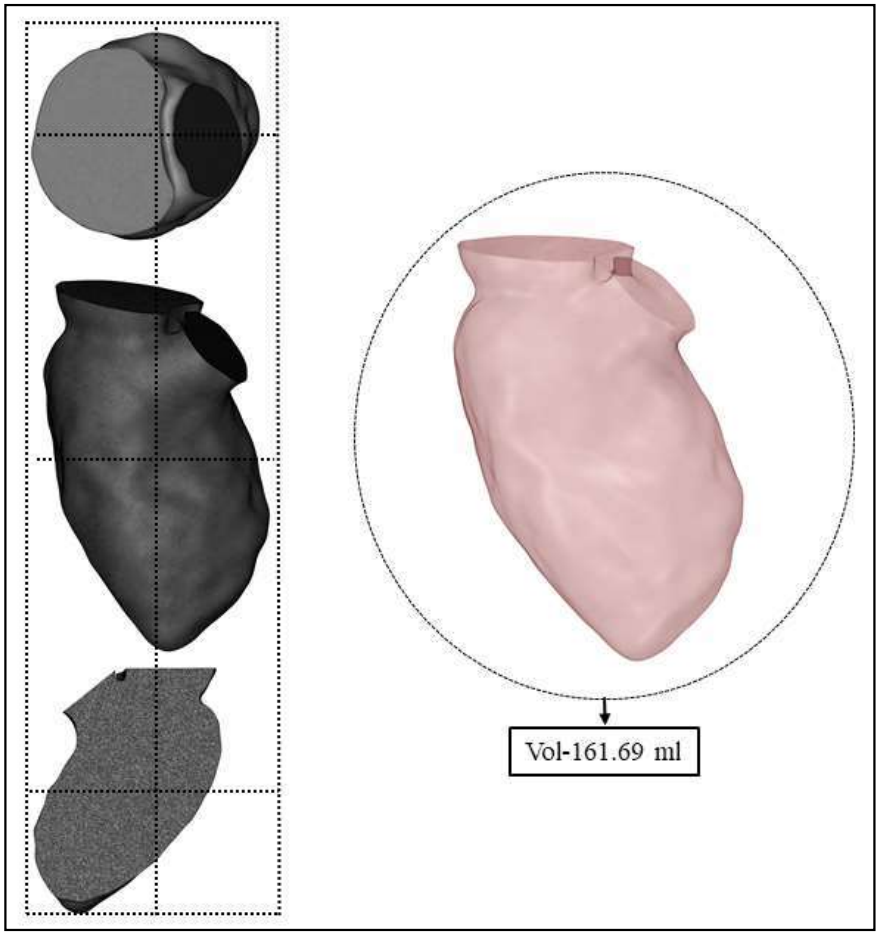

Figure 6.14: Meshing details, LV- M_1

Table.6.1 Meshing statics of Model_1

Model	Meshing Statics
M_1	Nodes - (79222), Faces - (152844)

6.2.3 Pulsatile boundary conditions

Here in this modelling approach, we used physiological pulsatile flow waveform as an inlet boundary condition and pressure waveform as shown in (Figure 6.15) at outlet to understand the blood dynamics in a physiological environment. Later on, we will shift

towards patient specific based boundary condition to accurately capture the flow dynamics according to patient geometry and flow and pressure waveform.

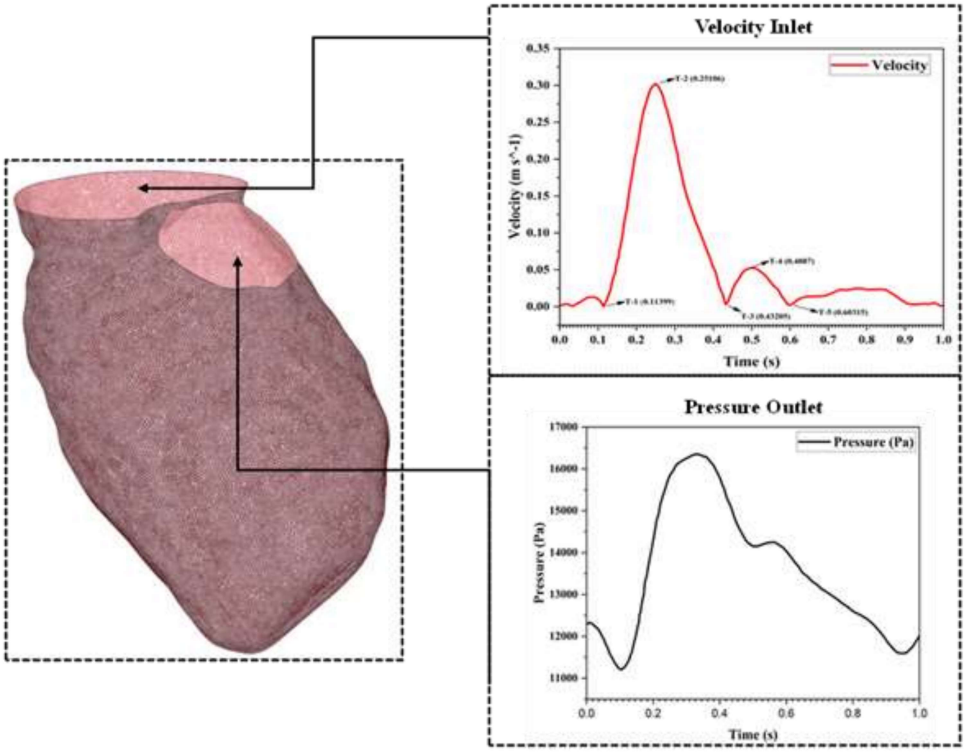

Figure 6.15 : Physiological Pulsatile flow condition (Kumar et al., 2022)

6.2.4 Numerical modelling

For computing the filling and ejection ratio of blood flow in the LV region, the arbitrary Lagrangian-Eulerian (ALE) formulation of the Navier-Stokes equations was employed. The continuity equation for volume (dV) and surface (S) in integral form:

$$\int_V \rho dV + \int_S \rho(\vec{v} - \vec{v}_b).\vec{n}\, dS = 0 \tag{1}$$

$$\int_V \frac{\partial}{\partial t}(\rho\vec{v})dV + \int_S \rho\vec{v}\,(\vec{v} - \vec{v}_b)\,.\vec{n}\, dS = -\int_S p\mathbf{I}.\vec{n}\, dS + \int_S \boldsymbol{\tau}.\,\vec{n}\, dS \tag{2}$$

(3)

$$\tau = \mu\,(\nabla v + \nabla v^{T})$$

Where is p denoting pressure; $\boldsymbol{I}$ denotes tensor, $\boldsymbol{\tau}$ represent viscous stress tensor, $\vec{\boldsymbol{v}}$ denote the velocity vector of fluid, $\boldsymbol{\mu}$ is the dynamic viscosity 0.0035 Pa.s, $\overrightarrow{\boldsymbol{v_b}}$ is representation of velocity vector of moving boundary; $\vec{\boldsymbol{n}}$ is the boundary of the control volume and whereas, $\boldsymbol{\rho}$ is the density 1060 kg/m^3.

6.3 Results & discussion

6.3.1 Velocity & Streamlines

The periodic solution for late diastolic and early systolic fluxes was discovered after three iterations of computation. The two-dimensional flow patterns produced from the Lagrange stream function on one longitudinal section are dissected and analyzed since the spiral flow patterns with vortices are quite complex. Several transverse planes, S-1, S-2, S-3, S_4, and S-5, respectively, are represent in (Figure 6.16). (Figure 6.16 (a)) displayed streamlines of the S-1 section at the early systolic and diastolic phases. The detailed analysis shows the different patterns of the vortex's formation at the bottom of the LV near the wall at the early systole, and the number of vortices is increased in the late diastole phase due to the blood washout process. (Figure 6.16 (b-3)) illustrate the velocity streamline patterns on the transverse plane. It has been observed that the high vortex formed on the S-2 and S-5 plane at the early systole and late diastolic phases.

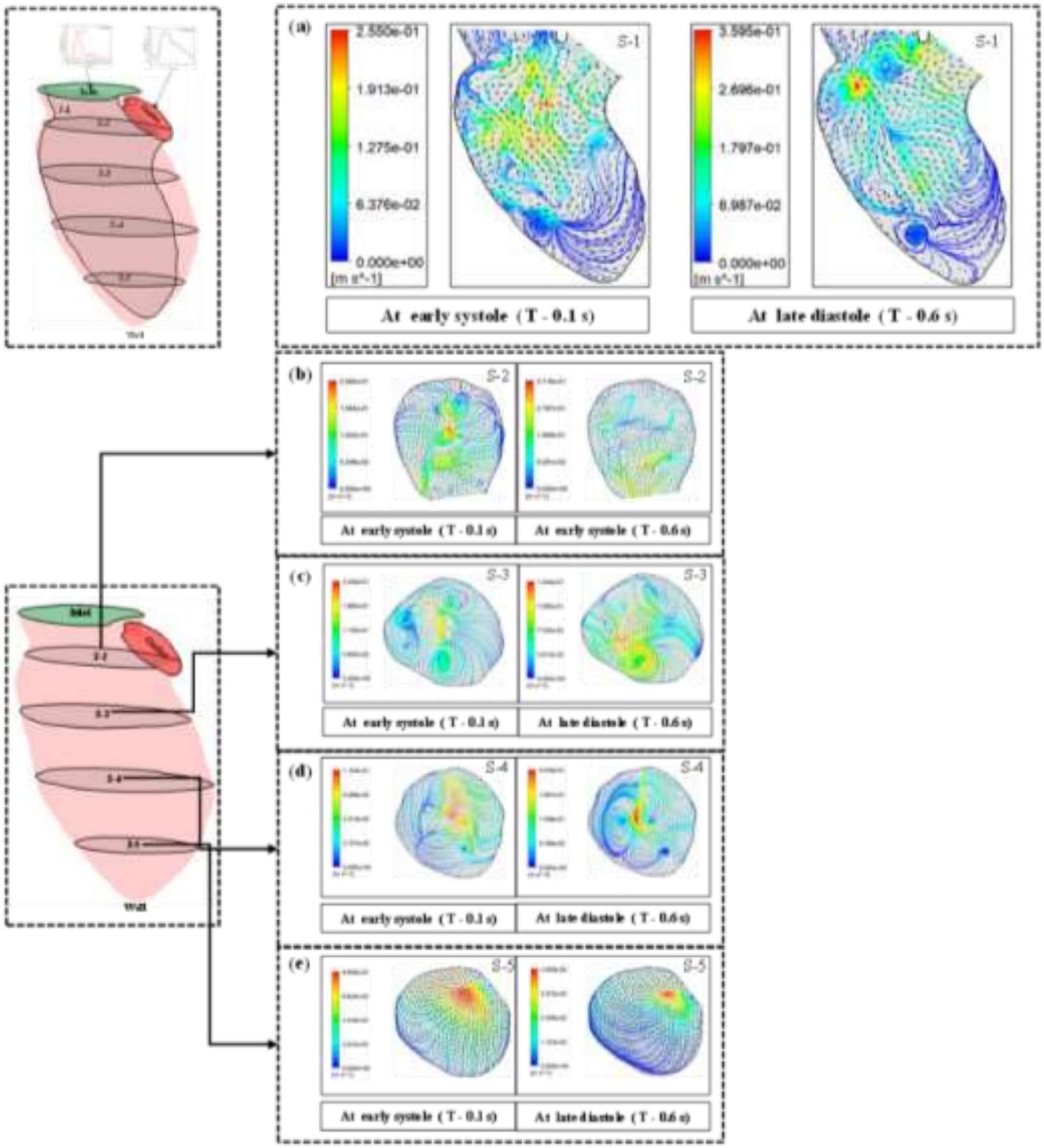

Figure 6.16 : Velocity streamlines of M-1 (a) On longitudinal plane S-1 at T-0.1s and T0.6s, Transverse plane (b) S-2, (c) S-3, (d) S-4 and (e) S-5 at T-0.1s and T-0.6s

6.3.2 Velocity contours of blood flow (M_1)

The blood flow volume of M_1 is 161.69 ml. (Figure 6.17) shows the velocity contours on the five sections of the LV model M_1 including the longitudinal and transverse planes at the early systole and the late diastole. (Figure 6.17) illustrates the velocity contour on the S-1 section, the maximum velocity value observed on the late diastole.

The value of maximum blood flow velocity on the transverse sections of LV models is shown in Figure 6.17 (b) & (c). According to the results observation, it has been shown that the value of maximum velocity 0.008 m/s occurs on the bottom section (S-5) of the M_1 model of LV.

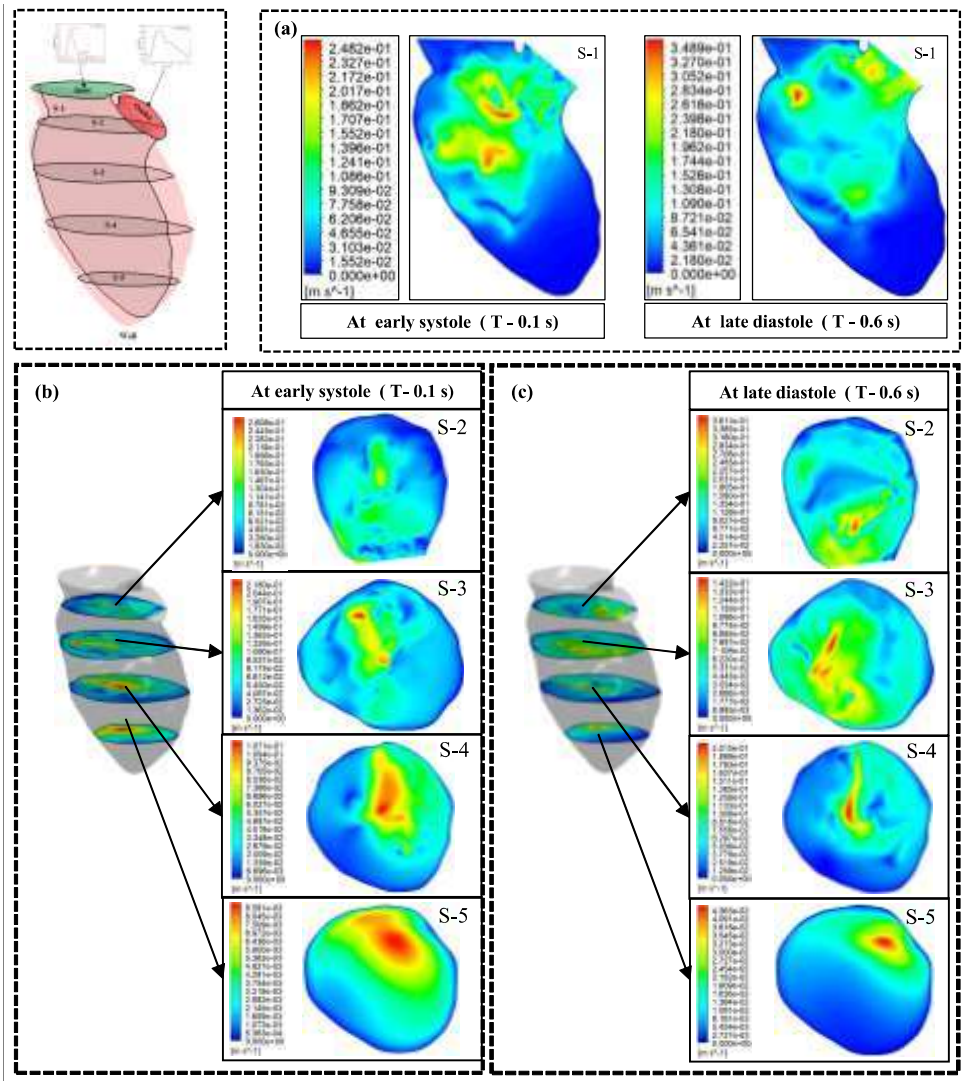

Figure 6.17 : Velocity contours of blood flow in model M_1 during T=0.1s & T= 0.6s

6.3.3 Wall pressure

Wall pressure results of left ventricle blood flow dynamics at early systole and late diastole as shown in (Figure 6.18). It is noted from the figure that the wall pressure on

model M_1s of LV during early systole, the wall pressure results during this phase can provide insights into the forces exerted by the blood on the ventricular walls. The value of maximum wall pressure at early systole is 11.2 KPa, which can show areas of high and low pressure on the ventricular walls. It has been observed that higher pressure near the regions of active contraction, such as the ventricular apex and outflow tract. These high-pressure regions can be important for assessing cardiac function and identifying potential areas of increased stress on the ventricular walls. These results provide the efficiency of blood filling, identifying any abnormal flow patterns or pressure gradients, and evaluating the overall diastolic function of the left ventricle.

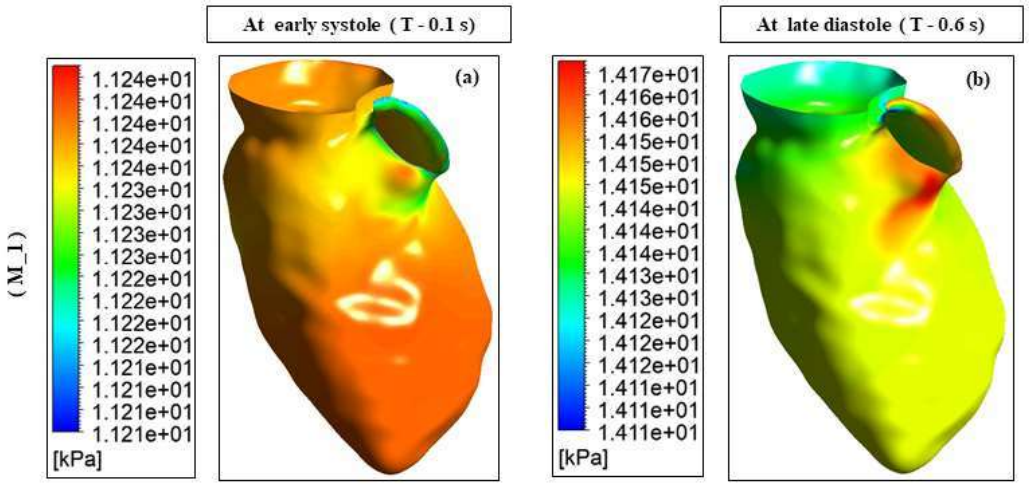

Figure 6.18 : Wall pressure (a) M_1 early systole and (b) M_1 late diastole

6.3.4 Wall shear stress

Wall shear stress (WSS) is crucial in understanding blood flow dynamics in the left ventricle (LV) during early systole and late diastole. It measures the frictional force employed by the circulating blood on the endothelial surface of the ventricular walls. Computational Fluid Dynamics (CFD) simulations can provide insights into the distribution of WSS during the cardiac cycle. WSS at early systole and late diastole are

shown in (Figure 6.19). The value of maximum WSS is 9.033e-03. The WSS results during this phase reflect the forces acting on the ventricular walls due to blood flow. WSS values are relatively lower compared to early systole due to the slower and more laminar flow patterns. However, localized variations in WSS can still occur based on the model's geometry and blood flow dynamics.

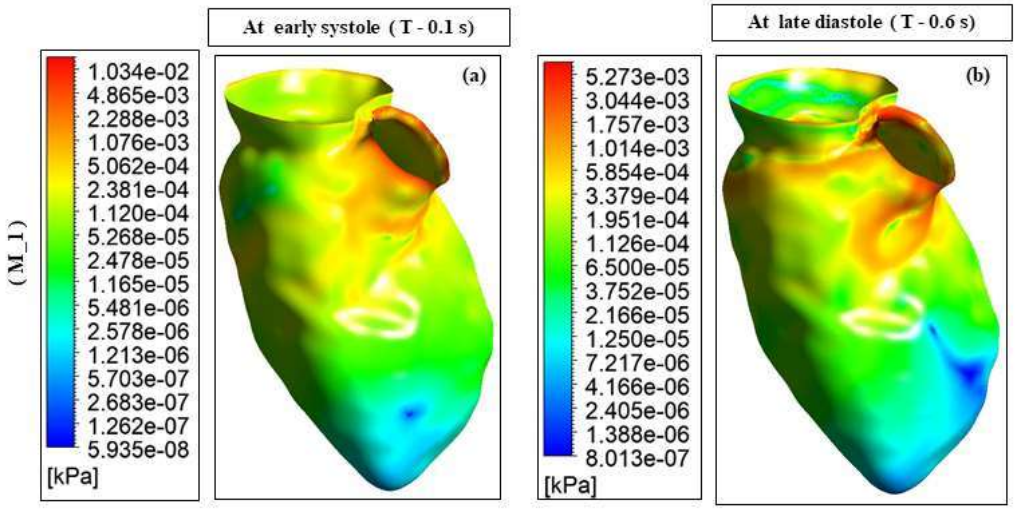

Figure 6.19 : Wall shear stress (a) M_1 early systole and M_1 late diastole

6.3.5 Vortex's core structures

In hemodynamic analysis of the LV using CFD, the Q criterion can be used to explain vortex structures (Kumar et al., 2023). Vortex structures are regions of swirling fluid motion that can be observed in the LV during the cardiac cycle. The Q criterion provides a quantitative measure to identify and characterize these vortices in CFD simulations. The three-dimensional vortex structure using the Q-criterion in four LV models at early systole and late diastole is shown in (Figure 6.20). It helps in identifying and quantifying the presence of vortices, which play a crucial role in understanding blood flow patterns, energy dissipation, and potential implications for cardiac function and disease progression.

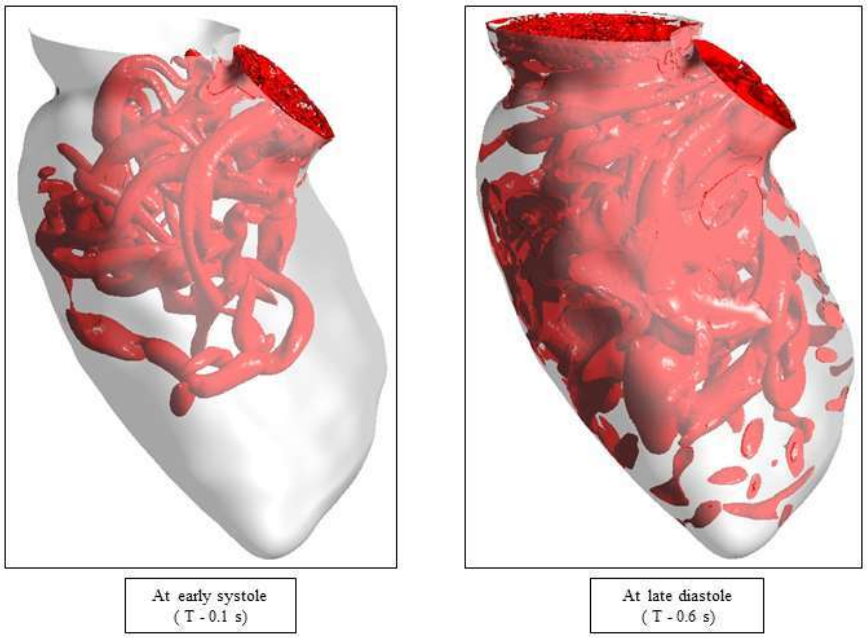

Figure 6.20 : The three-dimensional vortex structures using Q-criteria in model (M_1) of LV at early systole and late diastole

6.4 Summary

In summary, the hemodynamic study of the left ventricle (LV) using Computational Fluid Dynamics (CFD) provides valuable insights into the blood flow patterns and pressure distributions within the LV. CFD enables a detailed understanding of the cardiac function, which is crucial factor for the diagnosis and treatment of various cardiovascular diseases. The integration of patient LV anatomical features and physiological dynamics contributes to a realistic representation of blood flow patterns during the late diastole and early systole, where there is a relatively small variation in LV dimensions. The findings improve our understanding of LV hemodynamic and have the potential to assist in the diagnosis, treatment, and management of cardiovascular diseases like left ventricular hypertrophy (LVH) and planning for treatment like left ventricular assist device (LVAD). In summary, the application of

CFD to study LV hemodynamic offers significant potential in advancing our understanding of cardiac function, improving diagnostics, and guiding the development of innovative therapeutic approaches. Continued research in this field holds promise for enhancing patient care and promoting the development of personalized medicine in cardiovascular health.